

Effect of collision processes in divertor plasma on the tokamak operational window

¹D. Umezaki, ¹S. Yamoto, ²K. Hoshino, ¹N. Asakura, ¹N. Aiba

¹National Institutes for Quantum Science and Technology, Naka, Ibaraki 311-0193, Japan

²Faculty of Science and Technology, Keio University, Yokohama, Kanagawa, 223-8522, Japan

e-mail: umezaki.daisuke@qst.go.jp

This study focuses on the JT-60SA tokamak and analyzes the impact of large-angle elastic scattering (LES) and neutral-neutral collisions (NNC) on plasma transport using the integrated divertor code SONIC. To examine the operational window of the tokamak, we conducted a parametric scan of strike point positions, fuel gas puff rates Γ_{puff} , and radiation power P_{rad} using the improved SONIC code. The results have shown that NNC reduces ion density at the attach-detach boundary, where the peak heat load located. For $P_{rad}/Q_{out} \approx 50\%$, a gas puff rate $\Gamma_{puff} \geq 10 \times 10^{21} \text{ s}^{-1}$ was required to keep the peak divertor heat load below 10 MW m^{-2} . Scenarios with relatively higher strike point positions were found to be favorable for reducing the peak divertor heat load. The improved model provides insights into optimizing JT-60SA initial research phase experiment.

The reduction of the heat load on the divertor target is one of the most critical challenges to achieve long time operation of future fusion devices. The detached divertor plasma has been regarded as a standard approach to maintain low divertor heat load. The divertor detachment requires low electron temperature, achieved by impurity seeding and a fuel gas puff. A number of scrape-off layer and divertor simulation codes, such as SOLPS 4.0 [1] and SONIC [2], have been developed. The SONIC code consists of the Braginskii plasma fluid code SOLDOR, the steady state Monte Carlo (MC) neutral transport code NEUT2D, and the steady state MC impurity transport code IMPMC. The SONIC code has been applied to prediction of the JT-60SA plasmas and JA DEMO reactor design. While the code has been applied to analyze JT-60U experiments, it has overestimated the electron density profile at the outer divertor target by a factor of 2-3 [3]. In SONIC, the plasma transport perpendicular to magnetic field lines is modeled as an anomalous diffusion assumption, addressing the need to improve the plasma transport model [3]. Our previous study [4] has shown that additional plasma transport perpendicular to magnetic field lines can be driven by large-angle elastic scattering (LES) between fuel ions and fuel atoms, using a kinetic approach. Recently, a neutral-neutral collision (NNC) model utilizing a kinetic collision rate [5] has been implemented into the SONIC code [6]. Although the effect of NNC on particle exhaust in JT-60SA has also been investigated utilizing the DIVGAS code [7], no integrated code simulation incorporating NNC has been conducted for JT-60SA operations. In this study, the plasma transport model had been improved by implementing LES into the SONIC code. The aim of this research is to analyze the operational window for the initial research phase of JT-60SA by the improved SONIC code, which incorporates NNC and LES models. The analysis focuses on divertor heat loads and considers parameters such as the strike point position, gas puff rates (Γ_{puff}) and radiation power (P_{rad}).

In this study, the SONIC code is applied to the predictive simulation of initial research phase operation of JT-60SA. The input power from the core-edge boundary, Q_{out} , is set to $Q_{out} = 18 \text{ MW}$, equally distributed between deuteron ions and electrons. Deuterium gas puff is considered with gas puff rates of $\Gamma_{puff} = 5.0 \times 10^{21}$ to $20 \times 10^{21} \text{ s}^{-1}$. In this study, a simple radiation model [2] is employed for Ar and C impurity species, and thus the IMPMC code is not used. By adjusting the currents in the poloidal field coils, the strike point position at the divertor target can be modified. Using the above input parameters, the simulations of three different outer strike points have been conducted for the three cases with different outer strike point positions are performed. Figure 1 shows the positions of the strike points in the poloidal cross-section of the divertor region in each

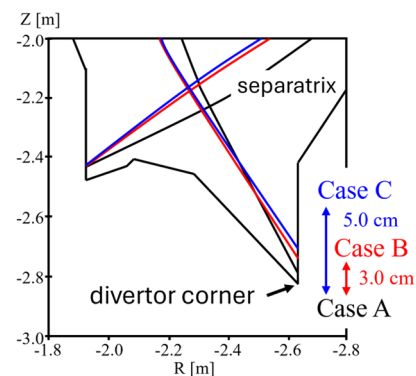


Fig. 1 Positions of strike points in the poloidal cross-section.

case. In Case A, the outer strike point position is 3.5 cm above the divertor corner. In Cases B and C, the outer strike points are located 3 cm and 5 cm higher than in Case A, respectively.

The plasma profiles at the outer target for Case B, at $P_{rad} = 9$ MW and $\Gamma_{puff} = 20 \times 10^{21} \text{ s}^{-1}$, are shown in figure 2(a) as a representative simulation result, where LES and NNC are considered. The horizontal axis represents the position on the divertor target, with the origin set at the strike point of Case A. In the region up to approximately 5.0 cm, the electron temperature T_e is sufficiently reduced, and thus the partially detached divertor is achieved at the outer target. The peak of divertor heat load is located at the attach-detach boundary 5–7 cm. Figure 2 (b) shows the ion density profile at the outer target with and without LES and NNC, along with the change ratio of ion density. At the attach-detach boundary (5–7 cm), the ion density decreased by approximately 5–10 %. The inclusion of NNC improves particle exhaust, leading to a decrease in ion density. When LES and NNC are considered separately, LES increases the density by 2–3%, while NNC decreases it by 12–13%. When LES and NNC are considered simultaneously, the combined rates of change are observed. As the gas puff rate increases, the neutral particle density became higher, and the density reduction effect caused by NNC became more pronounced. The above trend is also observed in Case C. In contrast, in Case A, the effects of LES and NNC on ion density were negligible, with the change ratio was only a few percent, likely due to the lower ion and atom densities. The above results suggest that the effects of LES and NNC can play a key role in deciding a preferable position of the strike point.

Figure 3 shows the dependence of the peak heat load at the outer target on gas puff rate for $P_{rad} = 9$ MW. In Cases B and C, as the gas puff rate decreases, the detachment area narrows, and the peak heat load increases significantly. This behavior arises because the divertor detachment in these cases is achieved by the reduction in electron temperature due to the increased plasma density associated with the gas puff rate. As seen from figure 3, a gas puff rate higher than $10 \times 10^{21} \text{ s}^{-1}$ is required to reduce the peak heat load below 10 MW m^{-2} . In addition, the magnetic configurations in Cases B and C are effective in achieving a low divertor heat load. As discussed earlier in this report, the LES and NNC have a non-negligible impact on the density profile at the outer target in Cases B and C. It should be noted that the same level of divertor heat load can be achieved in $P_{rad} = 13$ MW case with a lower gas puff rate. However, such high radiation power leads to high impurity accumulation. The density profile is crucial for assessing divertor detachment and divertor heat loads. The physical models newly introduced in this study could have an impact to assess the possible operation window of future tokamak devices.

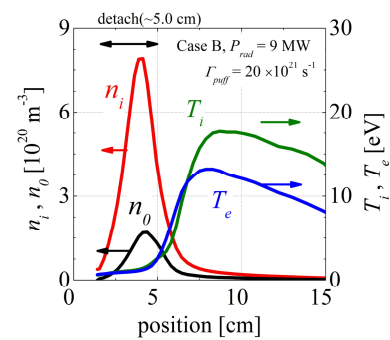


Fig. 2(a) The Plasma profiles n_i , n_o , T_i and T_e at $P_{rad}=9$ MW and $\Gamma_{puff} = 20 \times 10^{21} \text{ s}^{-1}$.

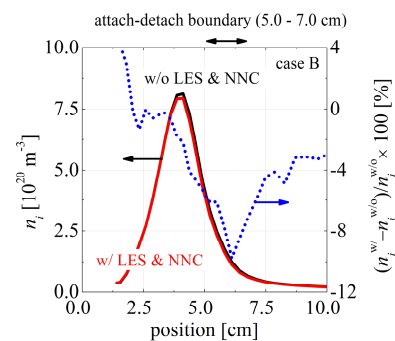


Fig. 2(b) The profiles of ion density (n_i) with and without LES and NNC, as well as the change ratio of n_i due to LES and NNC at $P_{rad}=9$ MW and $\Gamma_{puff} = 20 \times 10^{21} \text{ s}^{-1}$.

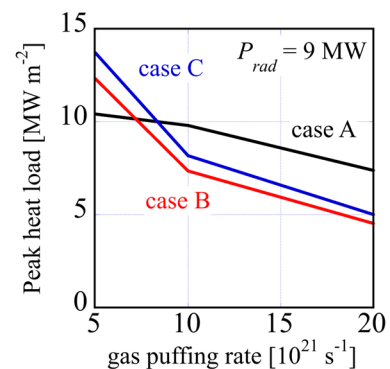


Fig. 3 The dependence of the peak heat load on the gas puff rate at $P_{rad}=9$ MW in each case.

- [1] A. S. Kukushkin, et al., *Fusion Eng. Des.* (2011), **86**, 2865.
- [2] H. Kawashima, et al., *Plasma Fusion Res.* (2006), **1**, 31.
- [3] K. Hoshino *J. Nucl. Mater.* (2015), **463**, 573.
- [4] D. Umezaki, et al., *Contrib. Plasma Phys.* (2024), **64**(1), e202300064.
- [5] P. Bechmann, et al., *Contrib. Plasma Phys.* (1995), **35**, 45.
- [6] S. Tokunaga, et al., *22nd International Conference on Plasma Surface Interactions in Controlled Fusion Devices*, P.3.105, May (2016), Rome, Italy.
- [7] C. Day, et al., the 26th IAEA Fusion Energy Conference, October (2016), Kyoto, Japan.